Field Consolidation of Varved Clay

Report No. 2

Richard P. Long, Associate Professor
Kent A. Healy, Associate Professor

Project 70-3 JHR 71-38
June 1971

Table of Contents

BISSELL BRIDGE AREA

The field observations from the Bissell Bridge area were analyzed using the techniques developed from the data for the East Hartford Expressway (1). The embankment went through two construction periods. The first period extended from late October to mid November 1956. The second period began in early January 1957 and lasted about a month.

During the first construction period a short, high embankment was built without berms and remained in place for approximately two months. The geometry of the fill for this period will be referred to as embankment-configuration-one. Sufficient piezometer and settlement platform data are available to evaluate apparent coefficients of consolidation, and initial and consolidation settlements under this loading.

In the second construction period, berms were added, the embankment was lengthened, and one part of it was lowered. The shape of the fill for this period will be referred to as embankment-configuration-two. Long term readings for some settlement platforms are available for this embankment configuration.

To insure that the techniques of data analysis developed for this project give accurate answers, the results are checked whenever possible. For the East Hartford Expressway, the evaluation of initial settlement from the square root of time plot compared well with the initial settlements computed from the observed settlements and percent consolidation. The Bissell Bridge data offered an opportunity to check the analysis techniques in more detail. The data from embankment-configuration-one yielded soil properties for this area pertinent to settlements. Settlements for embankment-configuration-two were predicted, using these soil properties, and compared with the observed long term settlements.

I. Data Analysis - Embankment-Configuration-One

A. Rate of Consolidation

The apparent coefficients of consolidation were evaluated from the rate of excess pore pressure dissipation using the entire isochrone from the piezometer groups at each of three settlement platforms; 3, 8 and 13. The dissipation pattern indicated double drainage. Only the excess pore pressure data from embankment--configuration-one were used. The method of evaluating the apparent coefficients of consolidation was basically the same as in the previous report (1). Embankment-configuration-one was completed about November 19, 1956. Piezometer readings in the supplied data were plotted to about mid December 1956, allowing the apparent coefficient of consolidation to be evaluated over a period of about a month. The earliest indication of berm construction was latter December 1956. The piezometer readings used in the analysis, therefore, were not affected by berm construction.

The piezometer readings after the fill was changed to embankment-configuration-two are difficult to interpret. For some time after rearrangement of the fill the top and bottom of the

the clay layer may have been swelling, while the center of the layer continued to consolidate.

The fill for embankment-configuration-one was applied continuously. With no pause in the filling sequence, the response of the piezometers to a distinct increment of fill could not be evaluated as at the East Hartford Expressway. The initial excess pore pressure isochrones were, therefore, computed using ICES-SEPOL. For all stress and settlement computations, the loads from the embankment configurations were approximated by a series of rectangular loaded areas placed upon each other as shown in Figure 1. The dotted lines represent the actual embankment. The solid lines show the profile of the rectangular loads. The natural ground slope across the centerline of the embankment was compensated for in the load approximation. Each rectangular loaded area has a width approximately the width of fill in the region it represents. The rectangular loads representing the top of the fill are narrower than those representing the bottom of the fill.

There are several methods of computing pore pressures by elastic theory. The three common methods tried at each piezometer location were: the normal stress in the vertical direction, the average normal stress, and pore pressure parameters with major and minor principal stresses. No laboratory data were available for the pore pressure parameters, but the assumption of parameters A and B equal to one gave reasonable values of initial excess pore pressures. The initial excess pore pressures were determined using the computed values of the principal stresses and the equation (2):

$$u = B \left[\sigma_3 + A(\sigma_1 - \sigma_3) \right] \quad . . . . \quad 1$$

With A and B both equal to one the pore pressure equals the major principal stress σ_1. Equation 1 gave values that agreed best with the field piezometer readings and was used to compute the initial excess pore pressure isochrones.

After the fill was complete, the shallowest piezometer showed less dissipation of excess pore pressure than the deeper piezometers. The shallow piezometers experienced a settlement of about one-half a foot or more by the end of filling which may have caused them to malfunction. To avoid an error due to the possible malfunctioning of these piezometers, the analysis used the lower half of each isochrone. Comparison of the coefficients of consolidation evaluated using the entire and the lower half isochrone only, showed little difference, probably because of the short observation period. The last isochrone used in the analysis was that of December 20, 1956, before any berms were begun. The percent consolidation was determined by comparing the area under each isochrone with the area under computed initial excess pore pressure isochrone and the apparent coefficient of consolidation evaluated as before (1). The results are shown in Table 1. The drainage at the Bissell Bridge is three dimensional, hence the higher values of C_{va}.

Table 1

BISSELL BRIDGE AREA
Embankment-Configuration-One

Settlement Platform Number	Apparent Coef. of Consolidation C_{va} (ft^2/day)	Initial Settlements (feet) from $\sqrt{t'}$ Plot	Initial Settlements (feet) from $\rho = \rho_1 + U\rho_c$	Consolidation Settlement (feet)	Total Settlement (feet)
3	5.3	0.35	0.40	0.80	1.05
8	5.2	0.88	0.88	1.0	1.88
13	10.5	0.27	0.22	0.58	0.85

B. Settlements

The data include field observations on 12 settlement platforms for embankment-configuration-one. The location of these platforms is shown in Figure 2. Settlement readings for platforms 3, 8 and 13, being close to piezometers, allowed an evaluation of the consolidation (ρ_c) as well as the initial settlement (ρ_i). Settlement data for the other nine platforms could be used to evaluate initial settlement only.

(1) Initial Settlements

Initial settlements for all settlement platforms shown in Figure 2 were evaluated by the square root of time method. The initial settlements are shown in Table 2 and in parenthesis in Figure 2. The initial settlement of platform 2 appears too large. The other initial settlements appear reasonable being greatest under the center of the fill and decreasing in both directions along the centerline.

In addition, the observations on settlement platforms 3, 8 and 13 were analyzed by the equation (1):

$$\rho = \rho_i + U\rho_c \quad . \; . \; . \; . \; . \; . \; . \; . \; . \; . \; . \; . \; . \quad 2$$

Initial settlements for platforms 3, 8 and 13 are also shown in Table 1. The values of initial settlement, determined by each method agree.

(2) Consolidation Settlements

Consolidation settlements were evaluated from Equation 2.

Table 2

BISSELL BRIDGE AREA
Embankment-Configuration-One

Settlement Platforms	Initial Settlements from $\sqrt{t}$ Plots (feet)
2	1.23
3	0.34
4	0.36
8	0.88
9	0.89
12	0.41
13	0.27
14	0.36
16	0.33
17	0.24
18	0.18
19	0.0

The results are shown in Table 1. The consolidation settlements show the same pattern as initial settlements, i.e., highest in the center of the embankment and decreasing in both directions along the centerline.

II. Data Analysis - Embankment-Configuration-Two

A. Comparison of Predicted & Observed Settlements

The field data available for the second embankment configuration consist of long term settlement observations and as-built cross sections. Using the cross sections, the load of the embankment on the soil was again approximated by a series of rectangular loads. Average soil properties, computed from the results of the analyses from embankment-configuration-one, were used to predict the settlements under embankment-configuration-two. The average values used in these computations were:

$$E_u = 4.97 \times 10^{-5} \ \text{lb/ft}^2$$

$$M_v = 0.283 \times 10^{-5} \ \text{ft}^2/\text{lb}$$

$$C_{va} = 7.0 \ \text{ft}^2/\text{day}$$

where E_u is the undrained Young's modulus, M_v is the modulus of volume compressibility and C_{va} is the apparent coefficient of consolidation. The modulus E_u was used in computing initial settlement. Both M_v and C_{va} were used in computing consolidation settlements.

The settlements predicted with these soil properties are compared with observed settlements in Table 3. The location of

Table 3

BISSELL BRIDGE AREA
Embankment-Configuration-Two

Settlement Platform No.	Initial Settlement ρ_1 feet (computed)	October 26, 1957 Predicted Consolidation Settlement ρ_c feet	October 26, 1957 Predicted Total (Predicted) Settlement ρ feet	October 26, 1957 Observed Total (Observed) Settlement ρ feet	May 14, 1958 Predicted Consolidation Settlement ρ_c feet	May 14, 1958 Predicted Total (Predicted) Settlement ρ feet	May 14, 1958 Observed Total (Observed) Settlement ρ feet	October 26, 1959 Predicted Consolidation Settlement ρ_c feet	October 26, 1959 Predicted Total (Predicted) Settlement ρ feet	October 26, 1959 Observed Total (Observed) Settlement ρ feet	$\frac{\rho - \text{observed}}{\rho - \text{predicted}}$
19	0.30	0.61	0.91	0.85	0.75	1.05	1.11	0.81	1.11	1.18	1.06
5	0.16	0.48	0.64	0.61	0.59	0.75	0.71	0.64	0.80	0.77	0.96
10	0.14	0.46	0.60	0.56	0.56	0.70	0.70	0.60	0.74	0.84	1.13
26	0.10	0.37	0.47	0.34	0.43	0.53	0.51	0.46	0.56	0.58	1.04
23	0.10	0.37	0.47	0.11	0.43	0.53	0.32	0.46	0.56	0.36	0.65
27	0.10	0.33	0.43	0.22	0.42	0.52	0.34	0.45	0.55	0.41	0.75
28	0.06	0.25	0.31	0.03	0.31	0.37	0.08	0.34	0.40	0.10	0.25
25	0.19	0.48	0.67	0.87	0.52	0.71	0.96	0.54	0.73	1.09	1.45
22	0.10	0.33	0.43	1.04	0.42	0.52	1.20	0.45	0.55	1.22	2.21
17	0.30	0.61	0.91	0.28	0.75	1.05	0.56	0.81	1.11	0.63	0.57

settlement platforms are shown in Figure 3. The results are arranged in three groups. The first group, settlement platforms 19, 5, 10, 26, 23, are close to the centerline of fill and show good agreement between predicted and observed settlements. The second group, settlement platforms 27 and 28, are closer to the edge of embankment and predicted values are larger than observed settlements. The third group, platforms 25, 22 and 17, have observed settlements that appear inconsistent with their location in the fill. Platforms 25 and 22 had large settlements, but are near the edge of the embankment. Platform 17 has a small observed settlement but is near the centerline of the fill.

Further Investigation on Determining Initial Settlement from Field Data

The two methods used to determine the initial settlement from field data of the East Hartford Expressway and Bissell Bridge were investigated further. See report on Phase I for details of the methods (1).

Each of these methods comes from the theory of consolidation developed by Terzaghi which assumes that the dissipation of excess pore pressures occurs in only one direction (2). These techniques yield reasonable results for initial settlement of varved clay under field conditions that allow pore pressures to dissipate in several directions. Further justification of their applicability to field situations seemed desirable. The investigation applied the same techniques to settlement curves predicted by theories assuming multi-dimensional drainage. To insure that the techniques are not limited to the varved clay of the Connecticut Valley, data from two published papers were plotted and found to yield results similar to those in the report on Phase I (1).

<u>The Method Using Excess Pore Pressures</u>

While the Terzaghi model assumes drainage in only one direction, subsequent models account for drainage in several directions (3). In the Terzaghi model, the average percent consolidation may be defined in either of two ways. One is to compare the average excess pore pressure at some time with the initial average excess pore pressure and compute the percent consolidation from the equation (2):

$$U = (1 - \frac{\bar{u}}{\bar{u}_o}) \times 100\% \quad . . . . \quad 3$$

where U is the average percent consolidation, $\bar{u}$ is the average excess pore pressure at some time "t" and $\bar{u}_o$ is the average initial excess pore pressure.

Another way of defining average percent consolidation in Terzaghi's theory is to compare the settlement at time "t" with the settlements at very long times. The ratio gives the percent consolidation thus:

$$U = \frac{\rho}{\rho_u} \times 100\% \quad . . . . \quad 4$$

where: ρ is the settlement at time "t" and ρ_u is the ultimate settlement which requires a very long time.

Each of these methods yields the same result with the one-dimensional model. In the two and three-dimensional models percent consolidation is defined by Equation 4 only. Mathematical treatment of consolidation in more than one dimension indicates that the total stress in the consolidating medium under the loaded area is not constant but varies as a function of time and space. The pore pressures under the loaded area may increase for a short time after the load is applied then decreases. This phenomenon, called the Mandel-Cryer effect, requires that the precise definition of consolidation be limited to the ratio of settlement described by Equation 4. The percent consolidation computed from excess pore pressures will always be in error to some degree. Davis and Poulos (6) investigated the magnitude of probable error from using excess pore pressure dissipation to compute percent consolidation in a three-dimensional case. Their study indicates a maximum error of 16 percent with most situations producing an error considerably smaller. The use of the rate of excess pore pressure dissipation to determine percent consolidation in most field situations appears reasonable.

<u>Use of the Square Root of Time Plot</u>

1. Validity of the Approach

   The use of the square root of time plot was also adopted from Terzaghi's one-dimensional theory. The adjustment of time for the construction period is an approach recommended by Taylor (2). The interpretation of laboratory consolidation data with a square root of time plot is a generally accepted method. Laboratory consolidation tests, however, satisfy the condition of one-dimensional consolidation. The plot of laboratory consolidation data against the square root of time shows a slight initial settlement often attributed to incomplete saturation. Were the sample completely saturated, the square root of time plot would extrapolate through the origin. Results from theories considering excess pore pressure dissipation in more than one direction yield to the same treatment.

Recently, Gibson et al (3) published theoretical curves for the consolidation of a clay layer with drainage of excess pore pressures in more than one direction. The published consolidation curves were replotted with average consolidation against square root of time factor "T". For this technique of analyzing field data to be valid, the theoretical points must lay on a straight line that extrapolates through the origin. These plots are shown in Figures 4 and 5. Figure 4 shows the theoretical plot for consolidation settlement of a strip load on a layer of limited thickness. Figure 5 shows the theoretical plot for consolidation settlement of a circular load on a similar clay layer. Both plots approximate a straight line through the origin.

Consolidation theories formulated and published to date include the assumption that the permeability is the same in all directions. Natural soil deposits seldom match this assumption; the horizontal permeability is usually greater than the vertical permeability. To investigate the validity of the square root of time plot in a situation with relatively high horizontal permeability, an approximate solution was tried using the model shown in Figure 6. Horizontal and vertical drainage on a point by point basis was simulated by the equation (2):

$$U_z = \left[1 - \left(\frac{u_h}{u_o}\right)\left(\frac{u_v}{u_o}\right) \right] \quad \ldots\ldots\ldots\ldots \quad 5$$

where: U_z is the percent consolidation at a certain point. The pore pressure resulting from horizontal drainage only is u_h. The initial excess pore pressure at the point is u_o and u_v is the pore pressure resulting from vertical drainage only, all taken at the same point. Each point on an isochrone was computed by Equation 5. The area under the isochrone was then planimetered and compared with the area under the initial excess pore pressure isochrone to determine the average percent consolidation (1). Plots of the average consolidation thus determined versus the square root of time are shown in Figure 7. Although the first point on each plot lies above the line, the remaining points form a straight line that extrapolates through the origin.

2. Error Analysis

Since the theoretical values for excess pore pressure dissipation in more than one direction only approximate a straight line when plotted against the square root of time, a study was made of the magnitude of possible error from using this method. A straight line was drawn through the points ignoring the initial point or two on each graph. These initial points are sometimes lost in field data because they may occur during construction time. The straight line was extrapolated to the vertical axis and the distance from the origin noted as percent consolidation. The results of this study are shown in Table 4. The study indicates that the initial settlement from this method may be slightly in error. The absolute magnitude of error depends on the ratio of the consolidation to initial settlement. The percent error will be large when the initial settlement is small relative to the consolidation settlement and vice versa.

Table 4

ESTIMATE OF PROBABLE ERROR IN INITIAL SETTLEMENT DETERMINED BY THE SQUARE ROOT OF TIME PLOT

Assumption $\rho_i \approx \rho_c$

Data from:		$\frac{h}{b}$*	C_v/C_h	Possible Error as Percent Consolidation Settlement	Shape of Loading
$\sqrt{T}$ vs. U	Gibson et al	0.2	1	+5%	Strip
"	[3]	0.5	1	+8.5%	Strip
"		1.0	1	+4%	Strip
"		1.0	1	+3%	Circular
$\sqrt{t}$ vs. U	(Computer Program)	2.0	5	+3%	Strip
"		2.0	12.5	-2%	Strip
"		2.0	25.0	-5%	Strip
"		2.0	1	-3%	Strip

*h = thickness of clay

b = one-half width of loaded area for strip footing and radius of loaded area for circular footing

The stress-path method is an attempt to overcome some of the difficulties in applying the theory of elasticity. Stress-strain properties of each layer of soil beneath the loaded area are measured in consolidated-undrained or unconsolidated-undrained triaxial tests. The tests begin with the sample at the in situ stresses and then loaded undrained to the level of stress that the surface loading will impose. The strain that the sample undergoes in the test is summed over the layer to determine that layer's contribution to the initial settlement. The contributions for each layer are added to find the settlement at the surface.

Finite element analysis is a technique that allows computation of deformation when the stress-strain relation for the material is non-linear. This method requires a new computer program for each field site. The soil mass is visualized as being made up of many small elements each of which has certain stress-strain properties depending on the stress level. The computations are made by solving a stiffness matrix, insuring that strains within the model are compatible.

Any method of computation is only as good as the soil data put into it. Accurate computation requires a detailed description of both at rest stress conditions and type of loading (7).

Some of the initial settlement data from the East Hartford Expressway were analyzed by elastic theory. The solution for a triangular loading intensity on an elastic medium supported by rigid base was used (8). Only the data from locations 13, 5, 6 and 7 were used because their loading configurations most closely approximated the theoretical model. The theory was used to compute the average undrained Young's modulus (E_u) for each location. The results of these computations are shown in Table 5.

Table 5

UNDRAINED MODULUS COMPUTED BY THEORY

Settlement Platform Location East Hartford Expressway	ρ_i $\sqrt{t'}$	from Exact Theory E_u comp. $\times 10^5$ lb/ft^2	from ICES-SEPOL E_u comp. $\times 10^5$ lb/ft^2
13	0.39	0.94	1.76
5	0.47	0.80	1.13
6	0.36	1.67	1.81
7	0.50	1.67	1.81

The backfigured undrained Young's Moduli (E_u) are of the same order of magnitude and vary by a factor of two. Some data from consolidated-undrained tests on the varved clay were reviewed. The data were for samples from boreholes, AA-B7, BB-B1, BB-B2 and AA-B6. The undrained modulus (E_u) from the lab tests is approximately one order of magnitude higher than that backfigured from the field data. Were this lab data used to predict initial settlement in the field by means of elastic theory, the predicted values would be too small. The prediction of initial settlement for varved clay will require additional study.

Additional Comments on Initial Settlements

When the rate of consolidation is slow or the magnitude of consolidation settlement is small, the settlement at the end of the loading period closely approximates the initial settlement. One should however bear in mind that during the process of consolidation the rate is highest during the initial stages. A seemingly small coefficient of consolidation may allow considerable consolidation settlement during filling. A comparison between the computed initial settlement and the settlement at the end of filling for the data from the East Hartford Expressway is shown in Table 6. The rate of consolidation for the varved clay is sufficiently high to require some technique to separate the initial settlement from the observed.

An important unresolved difficulty in predicting initial settlement is that of evaluating any strains due to plastic yielding of the soil within the foundation (9). These strains become more important as the imposed load approaches the ultimate bearing capacity but begin occurring at a much lower load level. To account for this type strain a finite element approach is required (7).

Table 6

COMPARISON OF INITIAL SETTLEMENTS WITH
OBSERVED SETTLEMENTS AT THE END OF FILLING

Piez. & Settlement Platform Location (East Hartford Expressway)	Initial Settlement ρ_i in ft.	Settlement at the end of filling
3	0.63	1.03
4	0.32	0.38
8	0.50	0.83
13	0.39	0.58
2	0.18	0.37
5	0.47	0.55
6	0.36	0.53
7	0.50	0.70
12	0.31	0.63

EAST HOCKANUM INTERCHANGE

Rate of Consolidation at STA. 95+00 and 100+00

The rates of consolidation were estimated from piezometer readings at Stations 95+00 and 100+00 of the East Hockanum Interchange. All piezometers, except the shallowest in each vertical line (designated "A" on drawings) showed an increase in reading with time after the filling ceased directly over the piezometers. The increased readings were probably due to filling nearby. To obtain an estimate of the apparent coefficient of consolidation under these conditions several assumptions were made. It was assumed that the A piezometer in each line was reading properly and that the influence of the construction operations on the piezometer readings at this depth was negligible. The pore pressures at the end of a stage of filling were assumed to be due to only that fill immediately above them. These readings were programmed into ICES-SEPOL with an assumed value of C_{va} and the readings for the A piezometer were predicted. The value of C_{va} was adjusted until the predicted and actual reading in A piezometer agreed within 3 percent. The results of this analysis are shown in Table 7. The values at Sta. 100+00 are higher than determined for other locations. Attention is directed to confidence limits estimated for this approach to be $\pm$50%. Since the A piezometer is close to the top of the clay strata, a large change in C_{va} causes little change in the predicted values of the piezometer reading. One must take this into account when evaluating these results. Hence the true value of C_{va} may lie within a wide range from the computed value. The computed values of C_{va} from East Hockanum are of the same order of magnitude as those computed from the data of the East Hartford Expressway, using the complete isochrone.

Table 7

APPARENT COEFFICIENTS OF CONSOLIDATION
EAST HOCKANUM INTERCHANGE

Location	C_{va} ft^2/day $\pm$50%
STA. 95+00 Line 2	
Piez. Line HR/P-5	0.343
STA. 100+00 Line 2	
Piez. Line HR/P-7	4.94
Piez. Line HR/P-8	4.25
Piez. Line HR/P-9	4.94
Piez. Line HR/P-10	3.98

LABORATORY TESTS ON VARVED CLAY

I. Consolidation Tests

A series of radial drainage consolidation tests were performed on samples of varved clay three inches high taken from 45 ft below ground surface, 300 feet south of the Charter Oak Bridge in East Hartford.

The samples were prepared for testing by cutting off a 3 inch length of the teflon-lined Shelby tube with the soil inside. A 3/16 inch diameter hole was cored through the center of the sample and filled with loose saturated sand. The samples were consolidated under the conventional loading sequence allowing drainage from the sand drain only. Consolidation was very rapid under these conditions (T_{90} < 3 mins.) and secondary compression prevented curve fitting techniques from being used to determine primary consolidation values accurately. It appears that the most reliable technique for calculating the rate of consolidation in the field under conditions of lateral drainage will be based on horizontal permeability measurements. A series of horizontal permeability tests will be run in the lab on undisturbed samples of the varved clay.

II. Initial Settlement

Analysis of the field data indicates that a substantial proportion of the total settlement of an embankment on varved clay occurs as the load is placed and is due to shear strains occurring with no volume change. Prediction of this shear settlement must rely on measurements of the shear modulus of the soil. Analysis of the field data has resulted in an apparent shear modulus of the varved clay. Laboratory triaxial tests will be run to measure the shear modulii of undisturbed samples and the values compared to the apparent field values.

REFERENCES

1. Long, R. P. and K. A. Healy, Preliminary Report, Field Consolidation of Varved Clay, Phase I, JHRAC, Project 70-3, JHR-PR 71-34, Jan. 1971. (This is Report No. 1.)

2. Lambe, T. W. and R. V. Whitman, "Soil Mechanics", J. Wiley and Sons, New York 1969.

3. Gibson, R. E., R. L. Schiffman and S. L. Pu, "Plane Strain and Axially Symmetric Consolidation of a Clay Layer on a Smooth Impervious Base," Quar. J. Mech. and Applied Math., pp. 505-520, Vol. 23, Part 4, Nov. 1970.

4. Spangler, M. G. and A. L. Griebling, "Foundation Settlement in the Ft. Randell Dam Embankment, NAS-NRC Highway Research Board Bulletin No. 173, 1958, pp. 1-19.

5. Lobdell, H. L., Settlement of Buildings Constructed in Hackensack Meadows, ASCE J. S.M. and Found., Vol. 96, No. SM 4, July 1970, pp. 1235-1248.

6. Davis, E. H. and H. G. Poulos, The Use of Elastic Theory for Settlement Prediction Under Three-Dimensional Conditions, Geotechnique, Vol. 18, No. 1, March 1968, pp. 67-91.

7. D'Appolonia, D. J. and T. W. Lambe, Methods for Predicting Initial Settlement, ASCE J. S.M. and Found., Vol. 96, SM2, March 1970, pp. 523-544.

8. Giroud, J. P. and A. Rabotel, Settlement of Embankment on Layer of Soil, ASCE J. S.M. and Found., Vol. 97, No. SM 1, Jan. 1971, pp. 287-293.

9. Meyerhof, G. G., The Tilting of a Large Tank on Soft Clay, Proc. South Wales Inst. of Engr., Vol. LXVII, No. 2, 1951, p. 53.

LEGEND FOR FIGURES

Figure 1 The approximation of the load due to embankment-configuration-one by rectangular loaded areas.

Figure 2 Location of settlement platforms for embankment-configuration-one.

Figure 3 Location of settlement platforms for embankment-configuration-two.

Figure 4 Plot of percent consolidation versus square root of time for two-dimensional case of a strip loading. Circular point represent theoretical points from paper by Gibson et al (3).

Figure 5 Plot of percent consolidation versus square root of time for circular loading, three-dimensional drainage.

Figure 6 Diagram of model used to compute consolidation for cases where horizontal permeability is greater than vertical.

Figure 7 Plot of results from the model shown in Figure 6. Top diagram for the case where $C_h = 12.5\ C_v$. Bottom diagram for the case where $C_h = 25\ C_v$.

Figure 8 Plots of field data from Ft. Randall Dam from Spangler (4).

Figure 9 Plots of field data from New Jersey varved clay from Lobdell (5). Maximum and minimum refer to settlements on the same building.

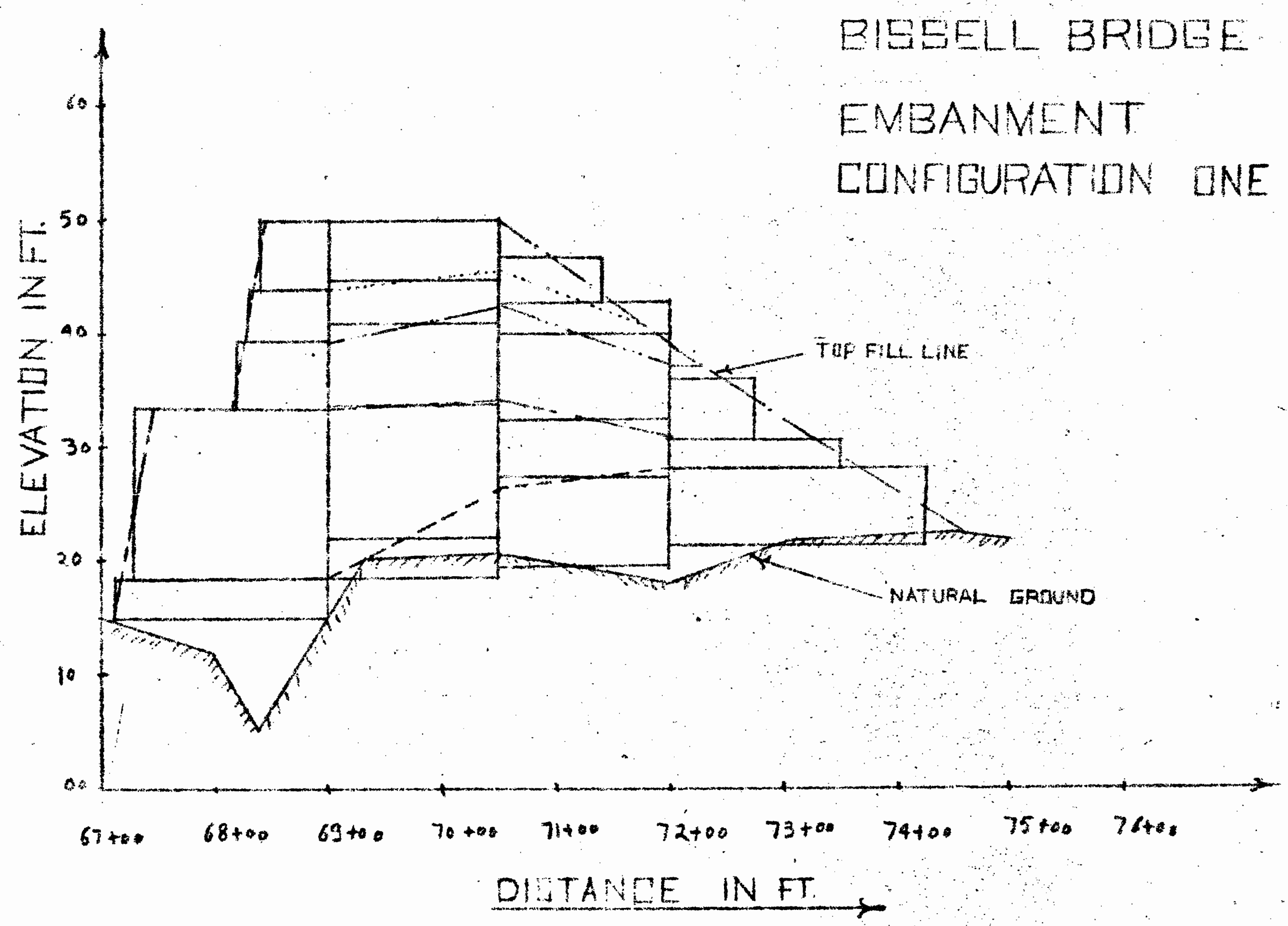

BISSELL BRIDGE
EMBANMENT
CONFIGURATION ONE
ELEVATION IN FT.
60
50
40
30
20
10
00
67+00
68+00
69+00
70+00
71+00
72+00
73+00
74+00
75+00
76+00
DISTANCE IN FT.
TOP FILL LINE
NATURAL GROUND

FIG. 1

LOCATION OF SETTLEMENT
PLATFORMS EMBANKMENT
CONFIGURATION ONE

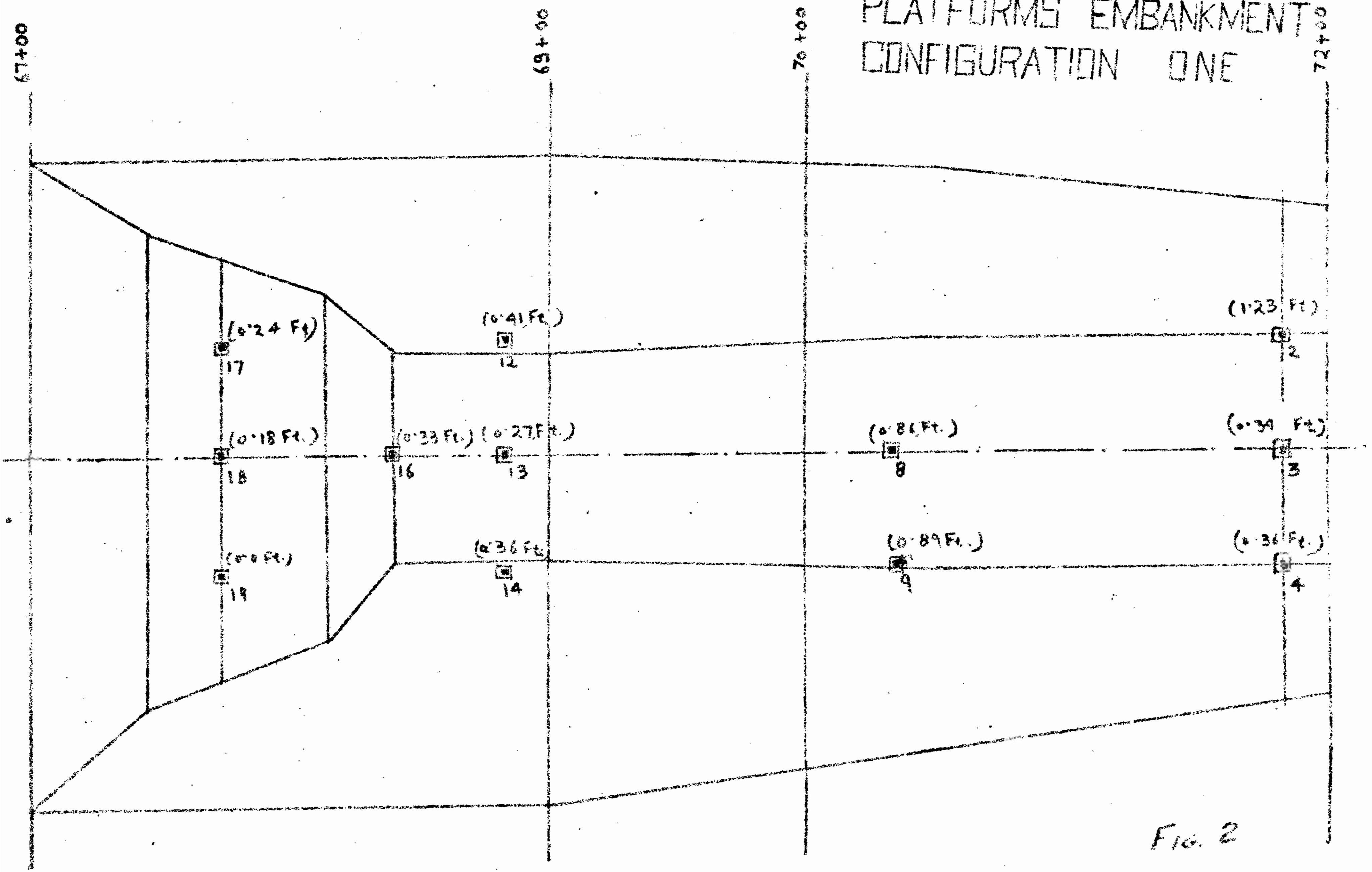

Fig. 2

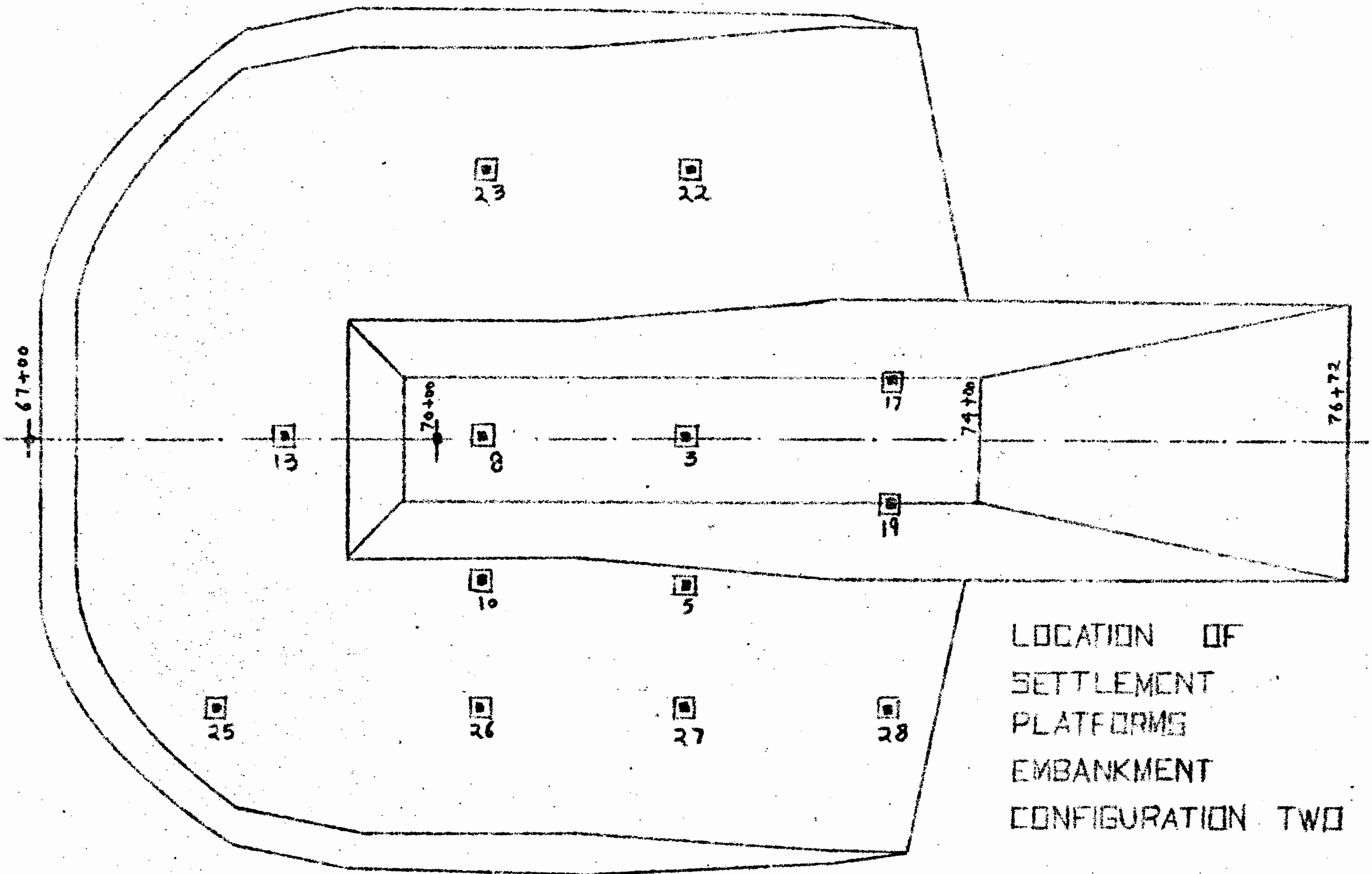

LOCATION OF
SETTLEMENT
PLATFORMS
EMBANKMENT
CONFIGURATION TWO

FIG. 3

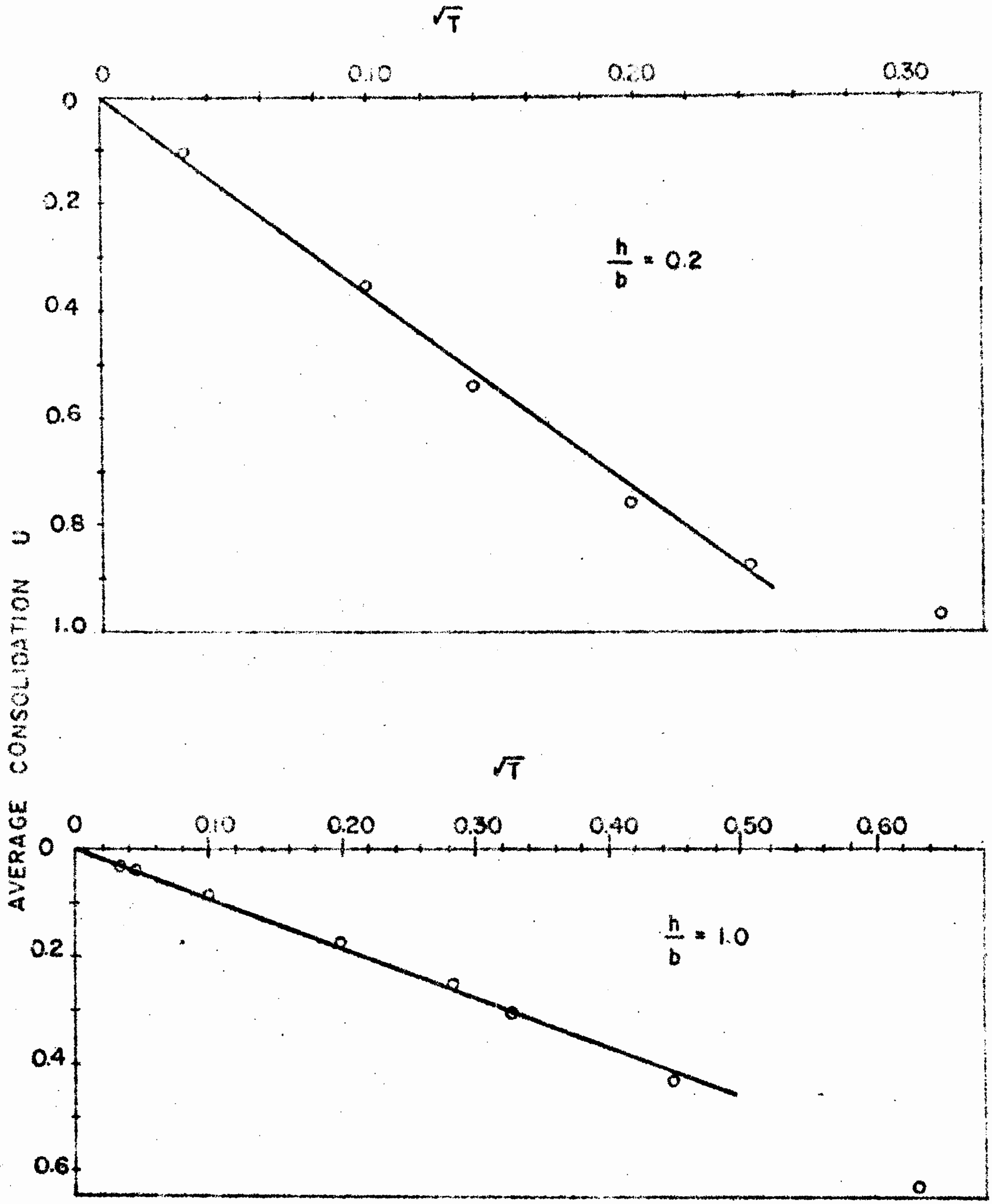

√T
0
0.10
0.20
0.30
0
0.2
0.4
0.6
0.8
1.0
h/b = 0.2
AVERAGE CONSOLIDATION U
√T
0
0.10
0.20
0.30
0.40
0.50
0.60
0
0.2
0.4
0.6
h/b = 1.0

FIG. 4

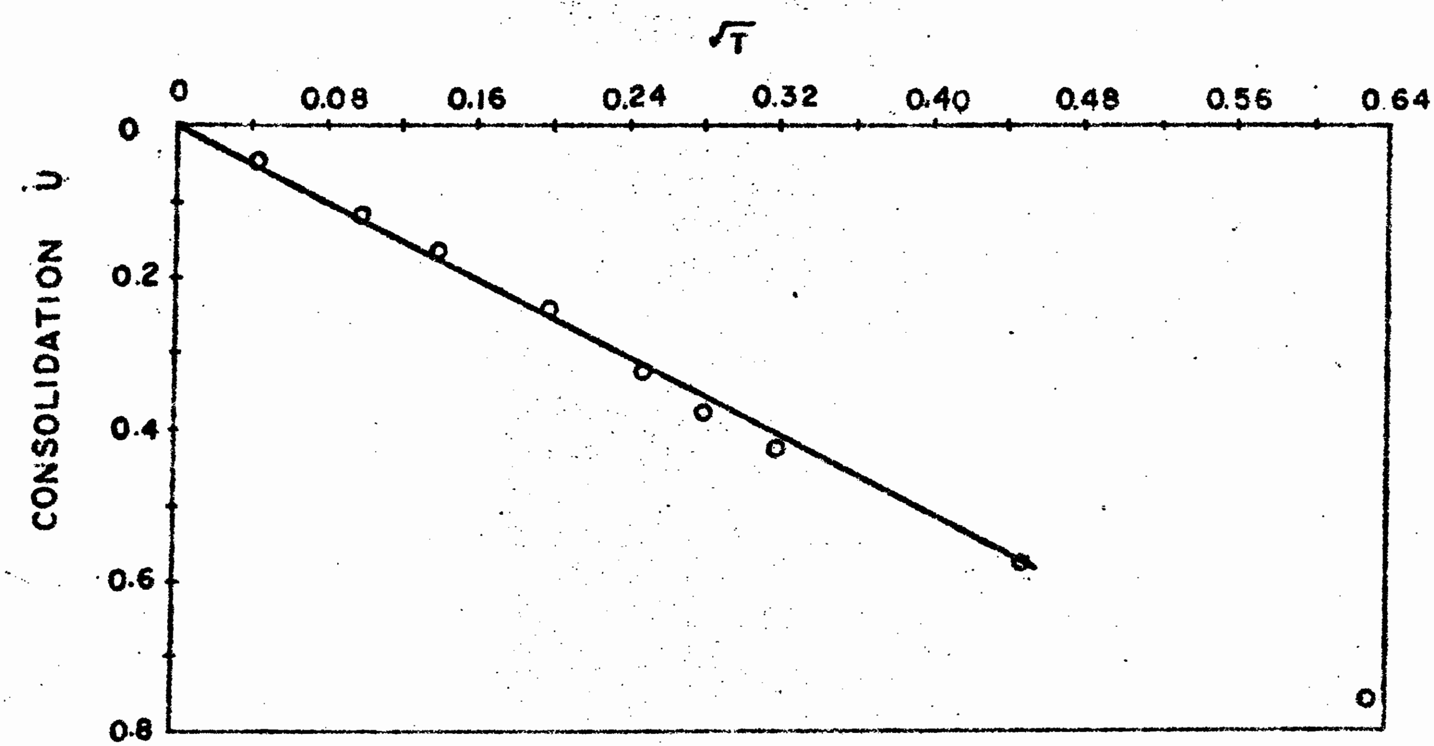

FIG. 5

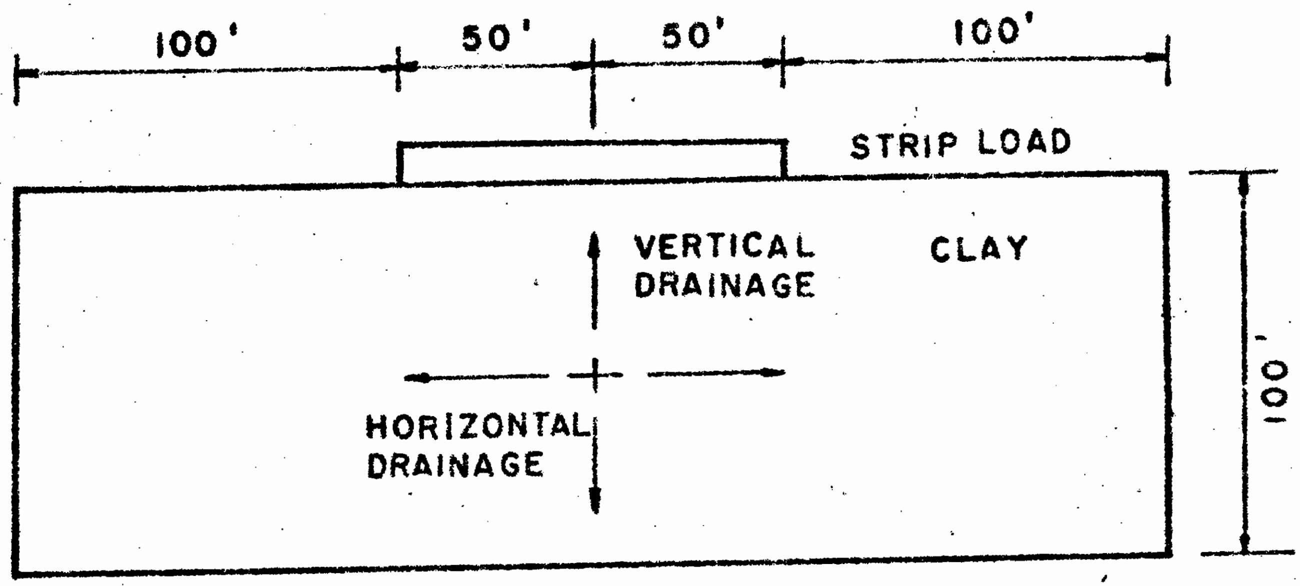

ALL BOUNDARIES CONSIDERED FREE DRAINING

FIGURE 6 MODEL USED FOR CONSOLIDATION UNDER VERTICAL AND HORIZONTAL PORE PRESSURE DISSIPATION.

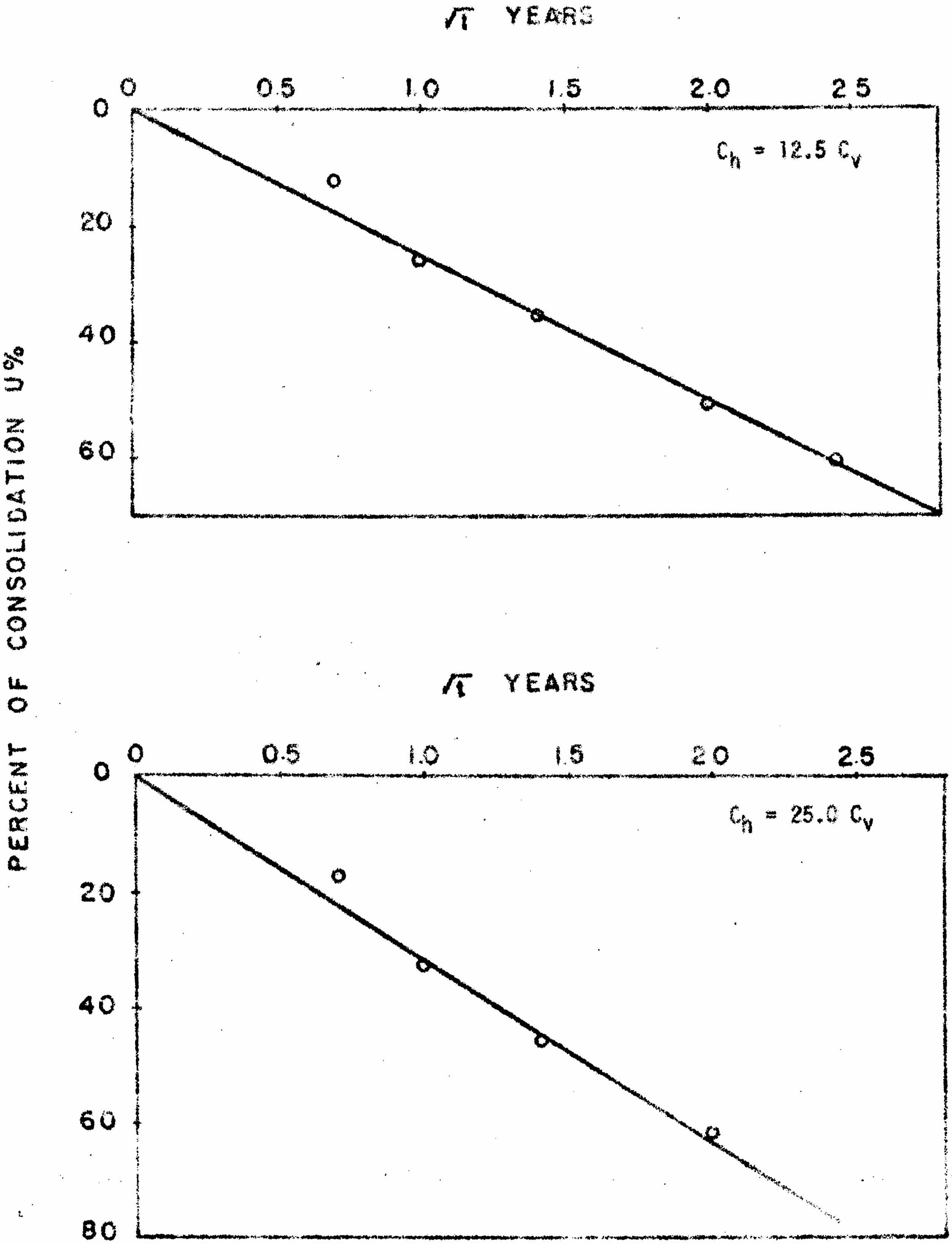

PERCENT OF CONSOLIDATION U%
√t YEARS
0
0.5
1.0
1.5
2.0
2.5
0
20
40
60
$C_h = 12.5\ C_v$
√t YEARS
0
0.5
1.0
1.5
2.0
2.5
0
20
40
60
80
$C_h = 25.0\ C_v$

FIG. 7

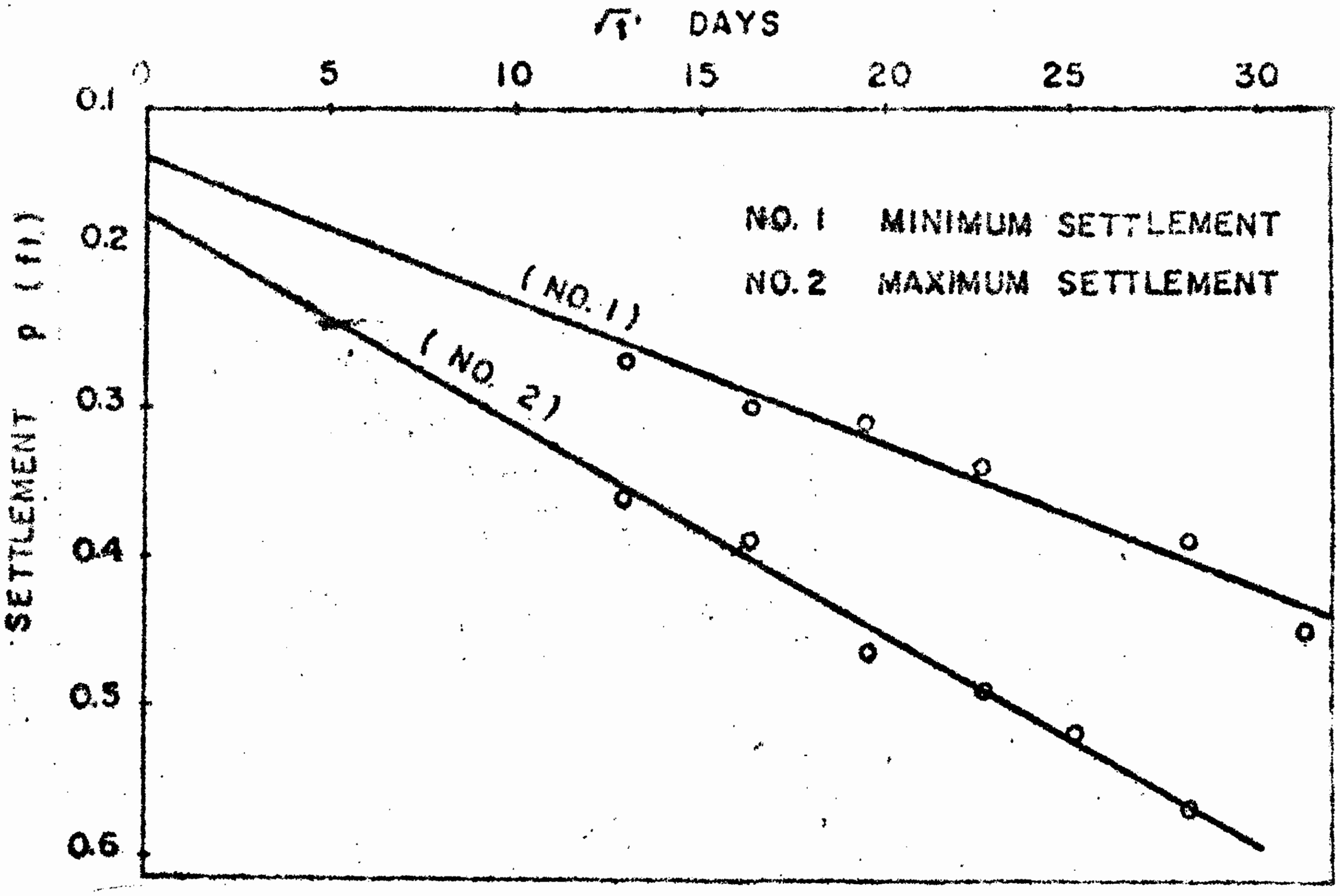

√t' DAYS
0
5
10
15
20
25
30
0.1
0.2
0.3
0.4
0.5
0.6
SETTLEMENT ρ (ft)
NO. 1 MINIMUM SETTLEMENT
NO. 2 MAXIMUM SETTLEMENT
(NO. 1)
(NO. 2)

FIG. 9a

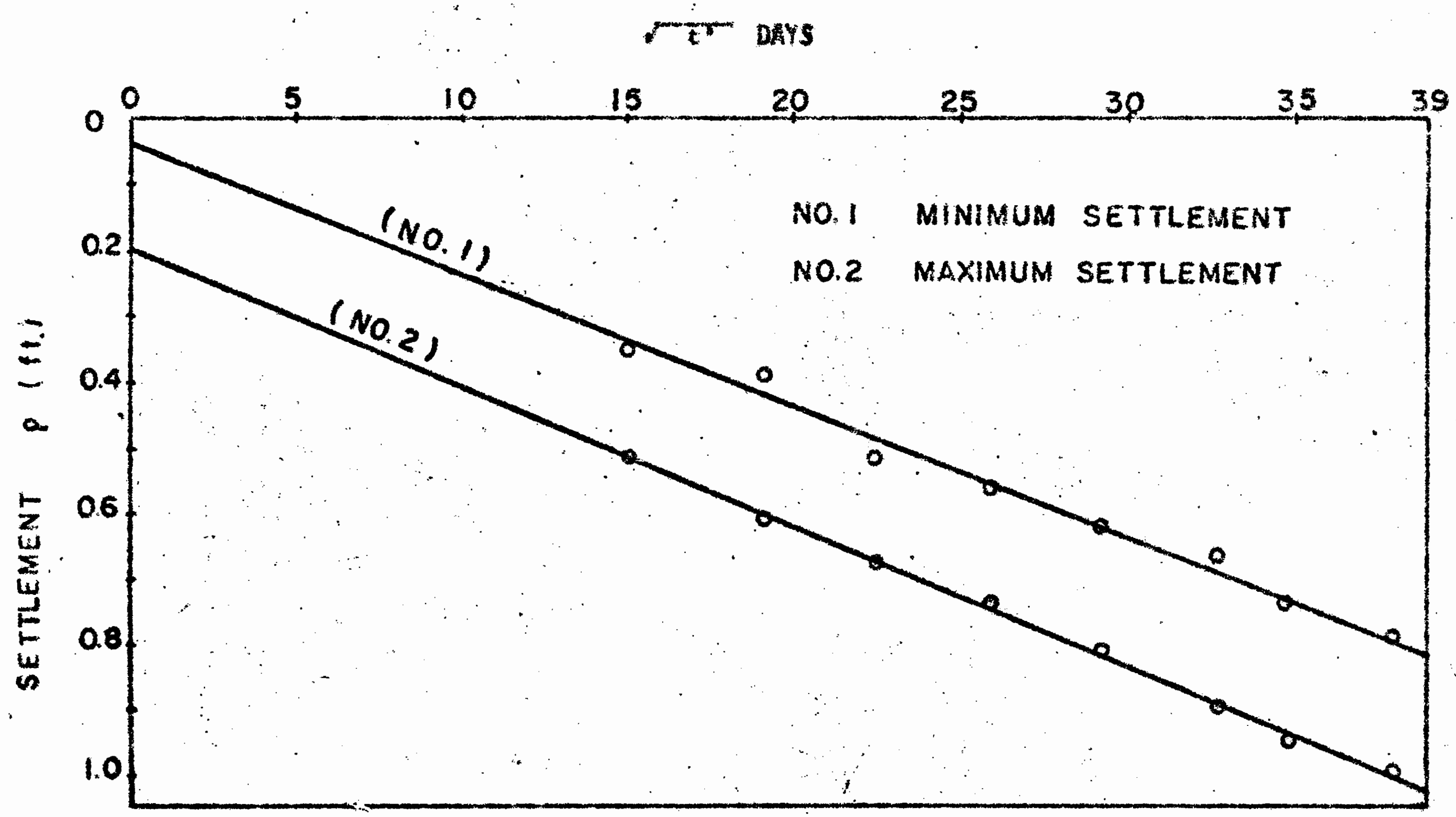
√t DAYS
0
5
10
15
20
25
30
35
39
0
0.2
0.4
0.6
0.8
1.0
SETTLEMENT ρ (ft.)
(NO. 1)
(NO. 2)
NO. 1 MINIMUM SETTLEMENT
NO. 2 MAXIMUM SETTLEMENT

FIG. 9b